J Solid State Electrochem (2012) 16:2623–2629
DOI 10.1007/s10008-012-1691-x

ORIGINAL PAPER

Surfactant-assisted electrodeposition and improved electrochemical capacitance of silver-doped manganese oxide pseudocapacitor electrodes

Montree Sawangphruk · Supree Pinitsoontorn · Jumras Limtrakul

Received: 16 December 2011 / Revised: 7 February 2012 / Accepted: 13 February 2012 / Published online: 23 February 2012

Abstract Ag-doped MnO_2 pseudocapacitor electrodes with dendrite and foam-like structures were successfully produced for the first time using an electrodeposition method employing structure-directing agents, i.e., sodium dodecyl sulfate (SDS) and cetyltrimethylammonium bromide (CTAB) acting through micelle formation at solid–liquid interfaces. Doping silver with MnO_2 enhanced their electronic conductance. Controlling pseudocapacitor electrode morphologies with surfactants accelerated ion transport. The specific capacitance values of the Ag-doped MnO_2 films produced with SDS and CTAB, measured in 0.5 M Na_2SO_4 at a scan rate of 5 mV s^{-1} were 551 and 557 $F g^{-1}$, respectively. These values are about 2.7-fold higher than that of the pure MnO_2 film and about 1.4-fold higher than that of the Ag-doped MnO_2 film made without using surfactants.

Keywords Electrodeposition · Supercapacitor · Pseudocapacitor · Manganese oxide · Surfactant · Electrochemical capacitance

M. Sawangphruk
Department of Chemical Engineering, Kasetsart University,
Bangkok 10900, Thailand

S. Pinitsoontorn
Department of Physics, Faculty of Science,
Khon Kaen University,
Khon Kaen 40002, Thailand

J. Limtrakul
Department of Chemistry and Center of Nanotechnology,
Kasetsart University,
Bangkok 10900, Thailand

M. Sawangphruk · J. Limtrakul
Center for Advanced Studies in Nanotechnology
and Its Applications in Chemical,
Food and Agricultural Industries,
Kasetsart University,
Bangkok 10900, Thailand

M. Sawangphruk (✉) · J. Limtrakul
NANOTEC Center of Excellence,
National Nanotechnology Center,
Kasetsart University,
Bangkok 10900, Thailand
e-mail: fengmrs@ku.ac.th

Introduction

Global warming and shortages of fossil fuels encourage society to move towards sustainable and renewable energies with low carbon emissions [1]. There is increasing interest in renewable energy. However, the lack of good electrical energy storage systems remains a large problem [1]. In order to overcome this problem, high-efficiency energy storage devices such as batteries and electrochemical capacitors (ECs) are needed. ECs are referred to as supercapacitors because of their extraordinarily high capacitance density. They can physically store charges at their solid–liquid interfaces. This phenomenon is known as electrochemical double-layer capacitance (EDLC). Thus, ECs does not produce any volume change that usually accompanies redox reactions of the active masses in batteries. The charging and discharging rates of ECs are equally high while those of batteries are kinetically limited since they rely on reaction kinetics and mass transport [2].

An important subclass of EC devices consists of pseudocapacitors which undergoes both an electron transfer reaction and EDLC storage. Materials that exhibit pseudocapacitive storage include conducting polymers [3] (i.e., polyaniline, polypyrrole, polythiophene, and poly(3,4-ethylenedioxythiophene) and a variety of transition metal

oxides. RuO_2 pseudocapacitors have relatively high specific capacitance (>1,000 Fg^{-1}) in this class. However, their costs are prohibitive and their materials toxic [4]. Efforts to develop more practical and inexpensive pseudocapacitive materials such as MnO_2 [5–9] and NiO [10–12] are now quite active. MnO_2 is an important and well-studied material for supercapacitors. It exhibits theoretical specific capacitance of approximately 1,110 Fg^{-1} through stoichiometric reduction of MnO_2 to MnOOH in a potential window of 1 V [13].

However, the capacitance for thick MnO_2 films (≈100 μm) is ultimately limited by the poor electrical conductivity of MnO_2. Alternatively, the stability of ECs in the thin MnO_2 film (<5 μm) configuration is restricted because of low mass loading [14, 15]. In order to overcome the electrical resistance of MnO_2, silver was incorporated into MnO_2 thin films. Ag mass loading of 50 μg cm^{-2} was accomplished using cathodic electrodeposition. This led to higher specific capacitance and lower electrical resistance compared with pure MnO_2 films. Specific capacitance of 770 Fg^{-1} was obtained for pure MnO_2 films at a scan rate of 2 mV s^{-1} in 0.5 M Na_2SO_4 electrolyte [6]. Previously, silver was incorporated in RuO_2 films using a radio frequency magnetron co-sputtering technique. The results showed that Ag-doped RuO_2 provided significantly higher specific capacitance than RuO_2 films. This was due to high electrical conductivity of Ag-doped RuO_2 [16].

In this work, we further improve the specific capacitance of Ag-doped MnO_2 films. This was done by controlling their morphology with surfactants in the electrodeposition process and increasing mass loading to an economical level (0.4–0.5 mg cm^{-2}) [17, 18]. Use of surfactants for controlling morphology of the electrodeposited Ag-doped MnO_2 has not been done previously. However, the effect of surfactants on the morphology of the pure MnO_2 films was previously studied. Adding surfactants (i.e., CTAB and Triton X-100) to the electrodepositing solution of manganese sulfate can increase the surface area of MnO_2. This leads to enhancement of the rechargeability of alkali manganese oxide batteries [19]. MnO_2 films electrodeposited in the presence of the Triton X-100 provide high porosity and therefore high surface area. This leads to 59% enhancement in specific capacitance when compared with values for MnO_2 film produced without Triton X-100 [5]. Structures of surfactants with nonpolar hydrocarbon chains and ionic or neutral polar head groups play an important role in electrosynthesis. This is because they can form micelle at solid–liquid interfaces [20–22]. Coulombic interactions between the head groups of surfactants and electrode surfaces are strong. Thus, micelles formed can be used as soft templates in the electrodepositing process [23].

Experimental

Chemicals and materials

Potassium permanganate ($KMnO_4$), silver nitrate ($AgNO_3$), sodium sulfate ($Na_2S_2O_3$), sodium nitrate ($NaNO_3$), potassium chloride (KCl), sodium dodecyl sulfate (SDS), cetyltrimethylammonium bromide (CTAB) purchased from the Sigma-Aldrich Co. were of analytical reagent grade. All solutions and subsequent dilutions were prepared using ultra-pure water (>18 MΩ cm). Graphite electrodes were supplied by Structural Probe, Inc.

Electrodeposition

Electrodeposition experiments were conducted using a conventional three-electrode system. A 1 cm^2 graphite substrate, a platinum mesh, and an Ag/AgCl electrode (in saturated KCl) were used as the working, counter, and reference electrodes, respectively. Electrodeposition of MnO_2 was performed following a reported cathodic electrodeposition [6]. We further developed the process as follows. The electrodeposition was carried out at a current density of 1 mA cm^{-2} vs. Ag/AgCl for 30 min in aqueous 20 mM $KMnO_4$ in 0.5 M $NaNO_3$ containing 0–1 mM $AgNO_3$ at 25 °C. The surfactants (CTAB or SDS) in concentrations of 0–1 mM were added to the process for the surface morphology-controlled samples. The as-electrodeposited films were annealed at 400 °C for 2 h to obtain a crystalline phase and to increase the purity of MnO_2 films [24].

Structural and morphological characterizations

The microstructure and composition of the as-prepared films were investigated using scanning electron microscopy/energy dispersive X-ray spectroscopy (EDX) operating at 15 kV. The XRD patterns of samples were recorded using a diffractometer with CuK_α radiation (λ = 1.5406 Å) and a graphite monochromator at 40 kV and 30 mA.

Electrochemical evaluation

Cyclic voltammetry (CV) and electrochemical impedance spectroscopy (EIS) were used to evaluate the specific capacitance and stability of as-prepared electrodes. These techniques used a computer-controlled μ-AUTOLAB II potentiostat (Eco-Chemie, Utrecht, The Netherlands) equipped with a FRA2 frequency response analyzer module running GPES/FRA software. CV curves were scanned at voltage ramp rates of 1–100 mV s^{-1}. EIS was carried out using a sinusoidal signal of 5 mV vs. Ag/AgCl over the frequency range from 100 kHz to 1 mHz. An aqueous electrolyte consisting of 0.5 M Na_2SO_4 was used for all

capacitive measurements. This was done because when applied to supercapacitors, aqueous Na_2SO_4 electrolyte, presents several advantages over the organic ones. It is relatively inexpensive, more environmentally friendly, and easier to make [25]. Additionally, the stability potential window of Na_2SO_4 with regard to the pseudocapacitive mechanism is about twice as large as in acidic or basic electrolytes [25].

Results and discussion

Surface morphology

Scanning electron micrographs of the Ag-doped MnO_2 films and the pure MnO_2 film are shown in Fig. 1. In the presence of a cationic surfactant, CTAB, agglomerated oxide nanoparticles with a foam-like structure were observed (Fig. 1a). With an anionic surfactant, SDS, a dendrite Ag-MnO_2 structure is seen (Fig. 1b). In contrast, without structure-directing surfactants, denser film structures were observed on both Ag/MnO_2 (Fig. 1c) and cracked MnO_2 (Fig. 1d) films. The crack-free morphology of Ag-doped MnO_2 is similar to materials recently reported [6]. This is possibly due to the strong interfacial interaction between the hybrid film and the graphite substrate. In contrast, the cracks typically found on the pure oxide films [26, 27] are because of the huge stress generated by the capillary force during the drying process [28, 29]. Surfactants significantly affect the morphology of the Ag-doped MnO_2 films. They play an important role in the nucleation and growth of hybrid films through the hemisphere-micelle formation at the electrode–liquid interface [19]. The structure of these products is controlled through a balance of interfacial forces between metal oxide precursor and surfactant [19, 30]. However, further studies on the nucleation mechanism for surfactant-assisted electrodeposition of foam-like and dendrite Ag-doped MnO_2 structures are still needed.

Chemical structure of silver-doped manganese oxides

The phase and purity of the as-annealed oxide films were determined by powder XRD measurements. The XRD patterns in Fig. 2a, b show five dominant peaks. They can be indexed as (110), (101), (111), (211), and (310) planes of a pure tetragonal phase of β-MnO_2 and are in good agreement with previous work [31, 32]. The XRD spectra also indicate that the films possess the high crystallinity of pure β-MnO_2. This is seen in the sharp and intense spectral peaks. Interestingly, in Fig. 2b, no peaks related to Ag are observed in Ag-doped MnO_2 samples. This can be attributed to Ag ion insertion inside the tunnel of the β-MnO_2 structure occurring more in doping than in the coating process. It is well established that MnO_2 can accommodate large ions such as

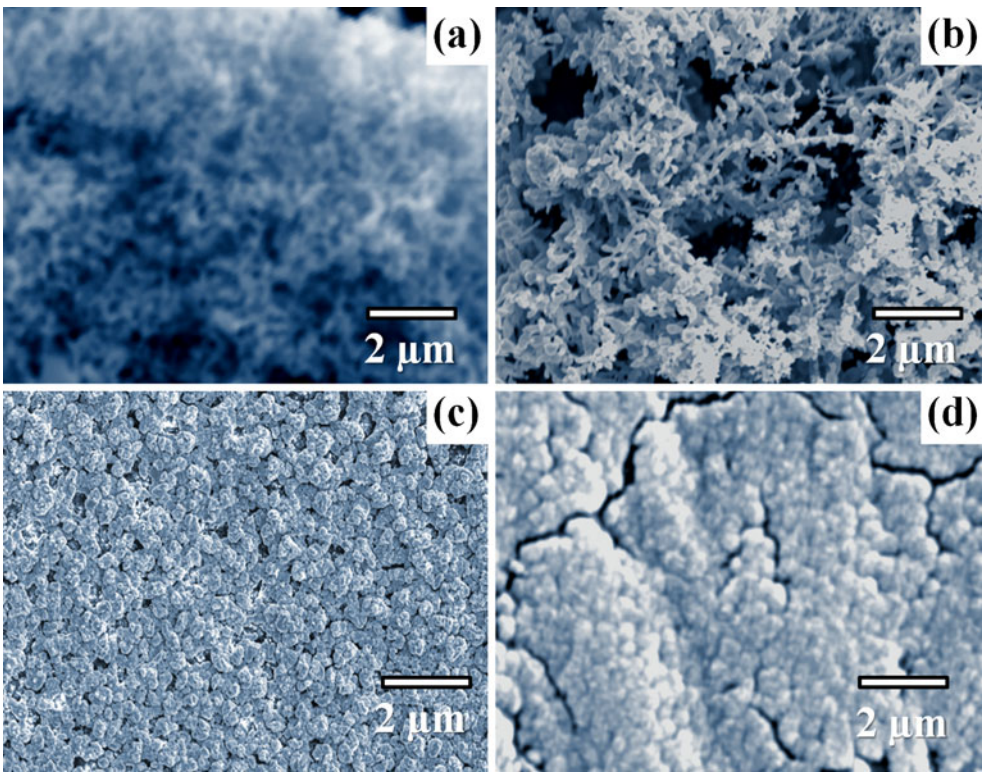

Fig. 1 Scanning electron micrographs of Ag-doped MnO_2 films produced using **a** CTAB, **b** SDS, **c** without surfactant, and **d** the pure MnO_2 film

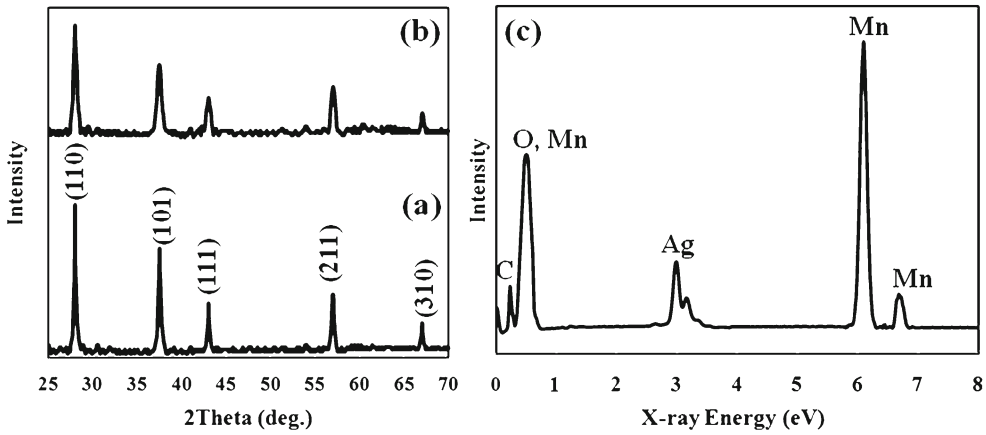

Fig. 2 X-ray diffraction patterns of **a** MnO_2 and **b** Ag-doped MnO_2 and **c** energy X-ray dispersive spectrum of Ag-doped MnO_2

Na^+, K^+, Ag^+, and Ca^{2+} [33–35]. Typical EDX spectrum of the Ag-doped MnO_2 films in Fig. 2c shows Mn, Ag, O, and C elements. A peak at 0.64 keV is attributed to $OL_{\alpha 1}$. Two peaks at 5.90 and 6.54 keV represent $MnK_{\alpha 1}$, and $MnK_{\beta 1}$, respectively. The two predominant peaks at 3.00 and 3.16 keV result from $AgL_{\alpha 1}$ and $AgL_{\beta 1}$, respectively. A peak at 0.28 keV is found associated with CK_{α} of the graphite electrode.

Electrochemical evaluation

Cyclic voltammetry

The EDLC of the Ag-doped and pure MnO_2 films was investigated by means of the cyclic voltammetry in a 0.5 M Na_2SO_4 electrolyte solution at potential intervals from 0 to 1 V vs. Ag/AgCl at the scan rate of 5 mV s^{-1}. The voltammograms indicate pseudocapacitive behavior which stores energy through highly reversible surface redox (Faradic) reactions and the EDLC with highly reversible charging–discharging reactions of cations (i.e., Na^+ and H^+) on the surface of oxide electrodes. The charge storage mechanism is attributed to the adsorption of Na^+ and H^+ on the surface of pseudocapacitor electrodes [14]. By integrating the cathodic current for all potentials and subtracting the capacitive current contributed by the substrate, a value of the pseudocapacitive current (I_{cv}) can be calculated. Using this value, along with the mass of deposition (m) and the scan rate (υ), we can then calculate the specific capacitance (C) according to the equation, $C=I_{cv}/m\upsilon$. From the CV in Fig. 3, the calculated C values of the Ag-doped MnO_2 electrodes produced using CTAB and SDS as soft templates, i.e., Ag/MnO_2 (CTAB) and Ag/MnO_2 (SDS) at the scan rate of 5 mV s^{-1} were 551 and 557 Fg^{-1}, respectively. These values are about 1.4- and 2.7-fold higher than that of Ag/MnO_2 and MnO_2, respectively.

CV measurements were also done at different scan rates over a range of 1–100 mV s^{-1}. Calculated C values are shown in Fig. 3b. These values decrease with increasing scan rates since the scan rate makes a direct impact on the diffusion of Na^+ and H^+ into the pseudocapacitor electrodes. At high scan rates, the cations (Na^+ and H^+) will primarily approach the outer surface of the electrode. At low scan rates, the cations can approach deep pores of the pseudocapacitor electrodes. Low scan rates allow more contribution to EDLC of the MnO_2. However, a closer look at the slope of the specific capacitance curves of the Ag/MnO_2(CTAB) and the Ag/MnO_2(SDS) electrodes in Fig. 3b is revealing that the diffusion of

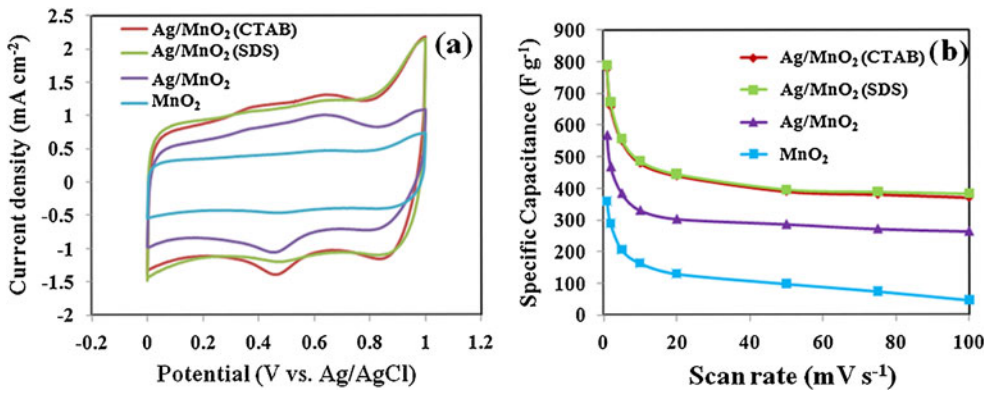

Fig. 3 **a** Cyclic voltammograms of the pure MnO_2 and Ag-doped MnO_2 films in 0.5 M Na_2SO_4 at a scan rate of 5 mV s^{-1} and **b** specific capacitance as a function of the scan rate for which Ag-doped films were prepared from 20 mM $KMnO_4$ solution containing 1 mM $AgNO_3$ and 1 mM surfactants (i.e., SDS or CTAB)

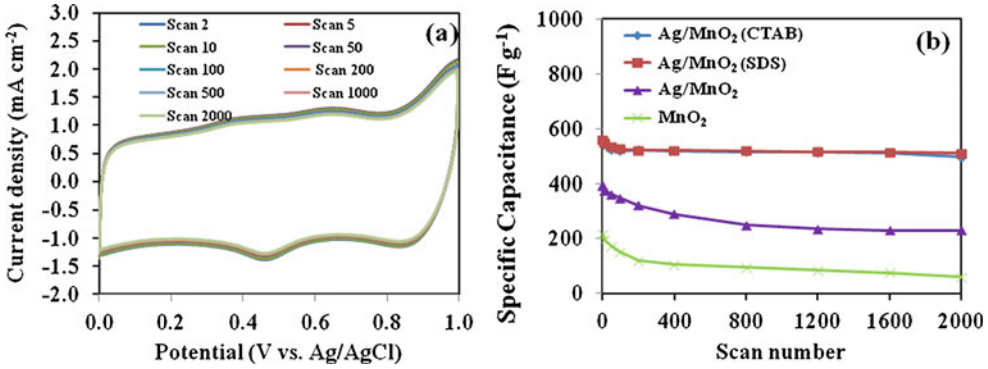

Fig. 4 **a** Cyclic voltammograms of Ag/MnO_2 (CTAB) at a range of scan (cycling) number (2–2,000) and **b** specific capacitance of all prepared films as a function of the scan number

Na^+ and H^+ inside deep nanopores at high scan rates can significantly enhance pseudocapacitance. This suggests that the foam-like structure of Ag/MnO_2(CTAB) and the dendrite structure of Ag/MnO_2(SDS) electrodes offer a faster pathway for ion transport and lower resistance for charge and electrolyte diffusion.

The stability of doped pseudocapacitors has additionally been studied using the CV measurements over scan (cycling) number of 2,000. Figure 4a presents CV curves of Ag/MnO_2 (CTAB) upon cycling for 2,000 scans at the scan rate of 5 mV s^{-1} with the cut-off voltages 0–1 V vs. Ag/AgCl in 0.5 M Na_2SO_4. The calculated value of C after 2,000 scans is only 1.4% less than that at scan number 2 (552 Fg^{-1}). This indicates high Ag/MnO_2 (CTAB) stability. Figure 4b compares the C values of all prepared films as a function of the scan number. In this figure, Ag/MnO_2 (SDS) with its dendrite structure provides similar C values over the scan number of 2,000 with high stability. This is comparable to Ag/MnO_2 (CTAB). However, the Ag/MnO_2 electrode made without surfactants in the electrodepositing process shows less specific capacitance (about 1.5 times). The C values of Ag/MnO_2 still possess a significant two- to threefold increase over that of pure MnO_2, which is in good agreement with very recent work [6].

Electrochemical impedance spectroscopy

The impedance plots in Fig. 5 show a partial semicircle at a high-frequency component. This is due to Faradic charge transfer resistance and a nearly straight line along the imaginary axis at a low-frequency component due to the mass transport limit. The smaller semicircles (inset of Fig. 5) in the high-frequency range are observed in the case of Ag-doped MnO_2 films. This can be compared with the larger semicircle of pure MnO_2. From this, it can be suggested that incorporation of silver into MnO_2 structure leads to fast electron transfer across electrified interfaces or an inner Helmholtz layer to the solvated cations in the outer Helmholtz layer. This process enhances the specific capacitance of pseudocapacitor electrodes as evidenced from the cyclic voltammetry. Additionally, the magnitude of charge-transfer resistances at the solid–liquid interface is in the following order: Ag/MnO_2(SDS)≈Ag/MnO_2(CTAB)<Ag/MnO_2<MnO_2. If charge-transfer resistance is smaller, the pseudocapacitor provides higher specific capacitance values [10]. The slope of the straight line in a low frequency range is due to the Warburg resistance. This is a result of the frequency dependence of ion diffusion from the electrolyte to the electrode interface. From the Nyquist curves, the slopes of the curves for the Ag/MnO_2 (SDS) and Ag/MnO_2 (CTAB) electrodes are steeper than the slope for Ag/MnO_2 and the pure MnO_2. This implies that the dendrite and foam-like structures of Ag/MnO_2 can significantly enhance diffusion of solvated cations to the porous electrodes. If we compared the Nyquist curves of Ag/MnO_2 and the pure MnO_2, doping silver into MnO_2 structure enhanced the electronic conductance of the oxide supercapacitor as well as the ion transport [36, 37].

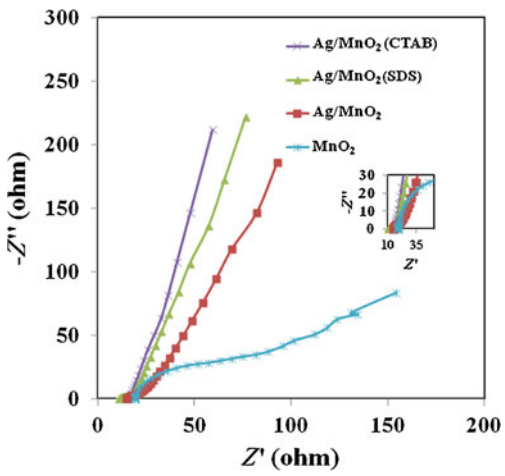

Fig. 5 Nyquist plots of as-prepared electrodes in 0.5 M Na_2SO_4 using a sinusoidal signal of 5 mV over the frequency range from 100 kHz to 1 mHz

Conclusions

In summary, MnO_2 and Ag-doped MnO_2 pseudocapacitors at a mass-loading level of 0.4 mg cm^{-2} were coated on graphite electrodes by using an electrodeposition. With the presence of surfactants (i.e., SDS or CTAB) in the electroplating solution, dendrite and foam-like structures of Ag-doped MnO_2 were successfully produced in lieu of denser films produced without surfactants in the solution. The specific capacitance values of the Ag/MnO_2 (CTAB) and Ag/MnO_2 (SDS) in 0.5 M Na_2SO_4 at the scan rate of 5 mV s^{-1} were 551 and 557 F g^{-1}, respectively. These values are about 2.7-fold higher than that of the pure MnO_2 and about 1.4-fold higher than that of the Ag-doped MnO_2 film without using surfactants. The foam-like structure of Ag/MnO_2 (CTAB) and the dendrite structure of Ag/MnO_2 (SDS) electrodes with high stability play an important role in the specific capacitance of pseudocapacitors by enhancing ion transport and lowering resistance for charge and electrolyte diffusion. These Ag-doped MnO_2 pseudocapacitor electrodes with foam-like and dendrite structures providing high specific capacitance and durability may be used for practical applications.

Acknowledgments This work was supported in part by grants from the Thailand Research Fund (MRG5480195), the National Science and Technology Development Agency (NSTDA Chair Professor and NANOTEC Center of Excellence), the Kasetsart University Research and Development Institute, the Commission on Higher Education, Ministry of Education ("the National Research University Project of Thailand" and "Postgraduate Education and Research Programs in Petroleum and Petrochemicals and Advanced Materials"). S.P. extends appreciation to the Integrated Nanotechnology Research Center, Khon Kaen University for their financial support.

References

1. Simon P, Gogotsi Y (2008) Materials for electrochemical capacitors. Nat Mater 7(11):845–854
2. Miller JR, Simon P (2008) Materials science—electrochemical capacitors for energy management. Science 321(5889):651–652
3. Snook GA, Kao P, Best AS (2011) Conducting-polymer-based supercapacitor devices and electrodes. J Power Sources 196 (1):1–12
4. Sugimoto W, Iwata H, Yasunaga Y, Murakami Y, Takasu Y (2003) Preparation of ruthenic acid nanosheets and utilization of its interlayer surface for electrochemical energy storage. Angew Chem Int Ed 42(34):4092–4096
5. Devaraj S, Munichandraiah N (2007) The effect of nonionic surfactant triton X-100 during electrochemical deposition of MnO_2 on its capacitance properties. J Electrochem Soc 154(10):A901–A909
6. Wang Y, Zhitomirsky I (2011) Cathodic electrodeposition of Ag-doped manganese dioxide films for electrodes of electrochemical supercapacitors. Mater Lett 65(12):1759–1761
7. Demarconnay L, Raymundo-Pinero E, Beguin F (2011) Adjustment of electrodes potential window in an asymmetric carbon/MnO_2 supercapacitor. J Power Sources 196(1):580–586
8. Zhu G, Li HJ, Deng LJ, Liu ZH (2010) Low-temperature synthesis of delta-MnO_2 with large surface area and its capacitance. Mater Lett 64(16):1763–1765
9. Sawangphruk M, Limtrakul J (2012) Effects of pore diameters on the pseudocapacitive property of three-dimensionally ordered macroporous manganese oxide electrodes. Mater Lett 68(1):230–233
10. Justin P, Meher SK, Rao GR (2010) Tuning of capacitance behavior of NiO using anionic, cationic, and nonionic surfactants by hydrothermal synthesis. J Phys Chem C 114(11):5203–5210
11. Gao B, Yuan CZ, Su LH, Chen SY, Zhang XG (2009) High dispersion and electrochemical capacitive performance of NiO on benzenesulfonic functionalized carbon nanotubes. Electrochim Acta 54(13):3561–3567
12. Nam SH, Kim YS, Shim HS, Choi SM, Kim HJ, Kim WB (2008) Size controlled nickel oxide nanoparticles on carbon nanotubes for supercapacitor electrode. J Nanosci Nanotechnol 8(10):5427–5432
13. Wu MS, Guo ZS, Jow JJ (2010) Highly regulated electrodeposition of needle-like manganese oxide nanofibers on carbon fiber fabric for electrochemical capacitors. J Phys Chem C 114 (49):21861–21867
14. Toupin M, Brousse T, Belanger D (2004) Charge storage mechanism of MnO_2 electrode used in aqueous electrochemical capacitor. Chem Mater 16(16):3184–3190
15. Pang SC, Anderson MA, Chapman TW (2000) Novel electrode materials for thin-film ultracapacitors: comparison of electrochemical properties of sol–gel-derived and electrodeposited manganese dioxide. J Electrochem Soc 147(2):444–450
16. Ahn H-J, Sung Y-E, Kim WB, Seong T-Y (2008) Crystalline Ag nanocluster-incorporated RuO_2 as an electrode material for thin-film micropseudocapacitors. Electrochem Solid-State Lett 11(7): A112–A115
17. Devaraj S, Munichandraiah N (2005) High capacitance of electrodeposited MnO_2 by the effect of a surface-active agent. Electrochem Solid State Lett 8(7):A373–A377
18. Chang JK, Tsai WT (2003) Material characterization and electrochemical performance of hydrous manganese oxide electrodes for use in electrochemical pseudocapacitors. J Electrochem Soc 150 (10):A1333–A1338
19. Ghaemi M, Khosravi-Fard L, Neshati J (2005) Improved performance of rechargeable alkaline batteries via surfactant-mediated electrosynthesis of MnO_2. J Power Sources 141(2):340–350
20. Matejka P, Vlckova B, Vohlidal J, Pancoska P, Baumruk V (1992) The role of triton X-100 as an adsorbate and a molecular spacer on the surface of silver colloid: a surface-enhanced Raman scattering study. J Phys Chem 96(3):1361–1366
21. Foucault R, Birke RL, Lombardi JR (2003) SERS of surfactants in monolayer and multibilayer forms on an electrified Ag surface. Langmuir 19(21):8818–8827
22. Ndiaye L, Cowache P, Cadene M, Lincot D, Vedel J (1993) Effect of a surfactant on cadmium telluride films prepared by electrodeposition on transparent conducting oxides. Thin Solid Films 224 (2):227–231
23. Rusling JF, Howe DJ (1994) Electron transfer in surfactant films on electrodes; copper phthalocyaninetetrasulfonate-didodecyldimethylammonium bromide. Inorg Chim Acta 226 (1–2):159–169
24. Nathan T, Cloke M, Prabaharan SRS (2008) Electrode properties of Mn_2O_3 nanospheres synthesized by combined sonochemical/solvothermal method for use in electrochemical capacitors. J Nanomater 2008. doi:10.1155/2008/948183
25. Demarconnay L, Raymundo-Pinero E, Béguin F (2010) A symmetric carbon/carbon supercapacitor operating at 1.6 V by using a neutral aqueous solution. Electrochem Commun 12(10):1275–1278
26. Babakhani B, Ivey DG (2011) Effect of electrodeposition conditions on the electrochemical capacitive behavior of synthesized

manganese oxide electrodes. J Power Sources 196(24):10762–10774
27. Broughton JN, Brett MJ (2005) Variations in MnO_2 electrodeposition for electrochemical capacitors. Electrochim Acta 50 (24):4814–4819
28. Gauthier G, Lazarus V, Pauchard L (2007) Alternating crack propagation during directional drying. Langmuir 23(9):4715–4718
29. Dufresne ER, Corwin EI, Greenblatt NA, Ashmore J, Wang DY, Dinsmore AD, Cheng JX, Xie XS, Hutchinson JW, Weitz DA (2003) Flow and fracture in drying nanoparticle suspensions. Phys Rev Lett 91(22):224501/1–4
30. Khimyak YZ, Klinowski J (2000) Formation of mesoporous silicates using Triton X surfactants in the presence of concentrated mineral acids. J Mater Chem 10(8):1847–1855
31. Yang Z, Zhou C, Zhang W, Li H, Chen M (2010) [beta]-MnO_2 nanorods: a new and efficient catalyst for isoamyl acetate synthesis. Colloids Surf A 356(1–3):134–139
32. Jia Y, Xu J, Zhou L, Liu H, Hu Y (2008) A simple one step approach to preparation of [gamma]-MnOOH multipods and [beta]-MnO_2 nanorods. Mater Lett 62(8–9):1336–1338
33. Abuzeid HM, Hashem AM, Narayanan N, Ehrenberg H, Julien CM (2011) Nanosized silver-coated and doped manganese dioxide for rechargeable lithium batteries. Solid State Ionics 182(1):108–115
34. Hu R, Cheng Y, Xie L, Wang D (2007) Effect of doped Ag on performance of manganese oxide octahedral molecular sieve for CO oxidation. Chin J Catal 28(5):463–468
35. Kunkalekar RK, Salker AV (2010) Low temperature carbon monoxide oxidation over nanosized silver doped manganese dioxide catalysts. Catal Commun 12(3):193–196
36. Zhang H, Yu X, Braun PV (2011) Three-dimensional bicontinuous ultrafast-charge and -discharge bulk battery electrodes. Nat Nanotechnol 6(5):277–281
37. Wang Y, Shi ZQ, Huang Y, Ma YF, Wang CY, Chen MM, Chen YS (2009) Supercapacitor devices based on graphene materials. J Phys Chem C 113(30):13103–13107